JOURNAL OF BACTERIOLOGY, July 2007, p. 4932–4943 Vol. 189, No. 13
0021-9193/07/$08.00+0 doi:10.1128/JB.00041-07

Characterization of a *Pseudomonas putida* Rough Variant Evolved in a Mixed-Species Biofilm with *Acinetobacter* sp. Strain C6▽

Susse Kirkelund Hansen,[1] Janus A. J. Haagensen,[1] Morten Gjermansen,[2] Thomas Martini Jørgensen,[3] Tim Tolker-Nielsen,[2] and Søren Molin[1]*

Infection Microbiology Group, BioCentrum-DTU, Technical University of Denmark, Building 301, DK-2800 Lyngby, Denmark[1]; Centre for Biomedical Microbiology, BioCentrum-DTU, Technical University of Denmark, Lyngby, Denmark[2]; and Optics and Plasma Research Department, Risø National Laboratory, Roskilde, Denmark[3]

Received 9 January 2007/Accepted 20 April 2007

Genetic differentiation by natural selection is readily observed among microbial populations, but a more comprehensive understanding of evolutionary forces, genetic causes, and resulting phenotypic advantages is not often sought. Recently, a surface population of *Pseudomonas putida* bacteria was shown to evolve rapidly by natural selection of better-adapted variants in a mixed-species biofilm consortium (S. K. Hansen, P. B. Rainey, J. A. Haagensen, and S. Molin, Nature 445:533–536, 2007). Adaptation was caused by mutations in a *wapH* homolog (PP4943) involved in core lipopolysaccharide biosynthesis. Here we investigate further the biofilm physiology and the phenotypic characteristics of the selected *P. putida* rough colony variants. The coexistence of the *P. putida* population in a mixed-species biofilm with *Acinetobacter* sp. strain C6 is dependent on the benzoate excreted from *Acinetobacter* during the catabolism of benzyl alcohol, the sole carbon source. Examination of biofilm development and the dynamics of the wild-type consortium revealed that the biofilm environment became oxygen limited, possibly with low oxygen concentrations around *Acinetobacter* microcolonies. In contrast to *P. putida* wild-type cells, which readily dispersed from the mixed-species biofilm in response to oxygen starvation, the rough variant cells displayed a nondispersal phenotype. However, in monospecies biofilms proliferating on benzoate, the rough variant (like the wild-type population) dispersed in response to oxygen starvation. A key factor explaining this conditional, nondispersal phenotype is likely to be the acquired ability of the rough variant to coaggregate specifically with *Acinetobacter* cells. We further show that the *P. putida* rough variant displayed enhanced production of a cellulose-like polymer as a consequence of the mutation in *wapH*. The resulting phenotypic characteristics of the *P. putida* rough variant explain its enhanced fitness and ability to form tight structural associations with *Acinetobacter* microcolonies.

It is frequently claimed that the vast majority of bacteria in natural settings live in surface-associated communities, also referred to as biofilms, and that such communities thrive on the presence of nutrients originating from the surfaces themselves or from the surrounding water (6, 12). Since most of these communities comprise multiple species, there will obviously be many instances of competition, commensalism, mutualism, synergy, parasitism, and other interactions between community members, and many of these will be driven by metabolic activities (7, 23, 32, 45, 49, 58). In structured communities, the heterogeneous distribution of biomass and of the various populations may allow the rapid development of nutrient gradients or opportunities for metabolic interactions, the consequence of which is that the actual spatial positioning of the various bacterial populations in relation to each other becomes an important ecological parameter (7, 19, 23, 46). In several documented cases, coaggregation of bacteria of different species seems to have evolved as an efficient strategy to optimize local opportunities (46). The best-studied case is that of the complex oral flora associated with dental plaque, where a very large number of species interact with each other to form a structured network of cells, which build up dental biofilms through numerous coaggregation events (30, 31). Some of these events seem to reflect metabolic interactions, thus documenting the assumptions indicated above. In the case of dental plaque, the microbial community is probably composed of the same groups of bacteria, which are naturally associated with the general oral flora, and many specific interactions, including coaggregation, have most likely evolved over a very long time. It is therefore not surprising that quite specific adherence factors have been identified as connecting cells of certain species to receptors present on surfaces of other specific cells (9, 10, 41). In other environments, where the conditions change more frequently, more stochastic interactions may be the rule, and in such cases specific coaggregation interactions may in fact be counterproductive. Instead, a diverse repertoire of structural interactions/coaggregations may be much more beneficial due to the flexibility provided by such ad hoc solutions. One such example of ad hoc association between two organisms has been characterized previously (7). A close association between environmental isolates of *Pseudomonas putida* R1 and *Acinetobacter* sp. strain C6 growing in flow chamber biofilms, with benzyl alcohol as the sole carbon and energy source, was observed. The driving force behind *P. putida* colonization of the *Acinetobacter* colonies seemed to be partial catabolism of benzyl alcohol by the latter organism resulting in excretion of benzoate, which was readily exploited by *P. putida* (37).

* Corresponding author. Mailing address: Infection Microbiology Group, BioCentrum-DTU, Technical University of Denmark, Building 301, DK-2800 Lyngby, Denmark. Phone: (45) 45 25 25 13. Fax: (45) 45 88 73 28. E-mail: sm@biocentrum.dtu.dk.

▽ Published ahead of print on 27 April 2007.

The flow chamber-based model system for studying biofilm formation and dynamics has the advantage of allowing online microscopic investigations of adaptive processes involving genetic changes (23). Evolved and wild-type (wt) genotypes can be reintroduced to the biofilm environment, and biofilm formation can be investigated under strictly controlled conditions (4). Eventually, such investigations may contribute to the understanding of the adaptation dynamics of more complex structured communities. Recently, we described the occurrence of evolution in a mixed-species biofilm consortium consisting of *Acinetobacter* sp. strain C6 and the laboratory strain *Pseudomonas putida* KT2440 growing on benzyl alcohol as the sole energy and carbon source (23). In this case, the *P. putida* strain was unable to degrade benzyl alcohol and was therefore totally dependent on the excreted benzoate. Genetic variants of *P. putida* appeared reproducibly, and the cause of this divergence was found (for a set of variants) to be mutations in a single gene (PP4943) homologous to the *wapH* gene of *Pseudomonas aeruginosa* PAO1 (35). These mutants had truncated core lipopolysaccharide (LPS) with the O antigen lacking (23) and a rough colony morphology, as often observed for core LPS variants (44). The *P. putida* rough colony variant was better adapted to the mixed-species biofilm environment, as shown by competitive fitness assays with the *P. putida* wt genotype. In addition, under conditions of very low levels of cross feeding, the derived variant was able to coexist with the *Acinetobacter* population, in striking contrast to the *P. putida* wt strain.

In the present study, we further investigate the structural interactions between *P. putida* KT2440 cells and *Acinetobacter* microcolonies in flow cell biofilms. We show that the consortium environment rapidly becomes oxygen limited, possibly creating conditions of low oxygen concentrations around *Acinetobacter* microcolonies. We further demonstrate that the *P. putida* wt population detaches from the biofilm in response to an oxygen downshift, indicating a possible explanation for the lacking structural interactions. In contrast, the *P. putida* rough variant displays a nondispersal phenotype in the mixed-species environment and forms coaggregates with *Acinetobacter*. Finally, we show that the *P. putida* rough variant has enhanced production of a cellulose-like polymer as a consequence of the core LPS mutation.

MATERIALS AND METHODS

Bacterial strains and culture conditions. The mixed-species biofilm consortium consisted of *Acinetobacter* sp. strain C6 (7) and derivatives of *Pseudomonas putida* KT2440 (17) without the TOL plasmid. The *P. putida* strains were the wt strain KT2440, with a *gfp* cassette inserted into the chromosome (SKH132), and a rough colony morphology variant (SKH208) derived from SKH132 by propagation for 10 days in a *P. putida-Acinetobacter* flow chamber biofilm (23). The rough variant was shown to have a spontaneous mutation in the *wapH* gene (PP4943) (TIGR Comprehensive Microbial Resource database [www.tigr.org]), which has a role in core LPS formation (23). In situ growth activity was visualized in the mixed-species biofilm population by using *P. putida* wt strain KT2440 with a mini-Tn*7*–Gm^r–*rrnB*P1–*gfp*[AAV] cassette (34) inserted into the chromosome (AKN142). *Acinetobacter* sp. strain C6 was grown at 30°C in Luria-Bertani (LB) broth or on LB agar. *P. putida* strains were grown at 30°C in AB minimal medium (11) supplemented with citrate (40 mM in agar or 10 mM in broth). Biofilms were cultivated using FAB medium (AB minimal medium with 10 μM Fe-EDTA replacing $FeCl_3$) containing benzyl alcohol (500 μM; Merck, Darmstadt, Germany) or benzoate (200 μM; Sigma Chemical Co., St. Louis, MO). FAB medium is composed of 1 mM $MgCl_2$, 0.1 mM $CaCl_2$, 0.01 mM Fe-EDTA, 15 mM $(NH_4)_2SO_4$, 33 mM Na_2HPO_4, 22 mM KH_2PO_4, and 51 mM NaCl. When required, antibiotics were added at final concentrations of 100 μg/ml of streptomycin, 10 μg/ml of gentamicin, and 10 μg/ml of kanamycin.

Cultivation of biofilms. Biofilms were grown in three-channel flow cells with individual channel dimensions of 1 by 4 by 40 mm. The flow system was assembled and prepared as described previously (8), with the modification of washing the system after sterilization with sterile milliQ water overnight. The substratum consisted of a microscope glass coverslip (st1; Knittel Gläser, Braunschweig, Germany). Each channel was supplied with a continuous flow of FAB medium containing the relevant carbon source. For propagation of mixed-species biofilm populations, flow cells were inoculated with a mixture of overnight cultures of *Acinetobacter* sp. strain C6 and *P. putida* KT2440 (wt or rough variant) diluted in a 0.9% NaCl solution. For monospecies biofilms, overnight cultures of the *P. putida* KT2440 wt or rough variant were used for inoculation. With arrested medium flow, the flow cells were turned upside down, and 250 μl of the diluted mixture was injected into each flow channel, using a small syringe. After 1 h, the flow cells were turned upside down, and the flow was resumed at a constant flow rate of 3.3 ml/h, using a Watson Marlow 205S peristaltic pump (Watson Marlow Inc., Wilmington, MA). After inoculation, each flow chamber contained ~2×10^6 CFU of *Acinetobacter* and ~2.5×10^5 CFU of *P. putida* (wt or rough variant) for mixed-species biofilms and ~2.5×10^5 CFU of *P. putida* for monospecies biofilms. The mean flow velocity in the flow cells was 0.2 mm/s. Biofilms were grown at 24°C. When possible, *Acinetobacter* sp. strain C6 was visualized prior to image acquisition by staining the biofilm with a 0.1% solution of Syto62 (Molecular Probes Inc., Eugene, OR) in FAB medium containing 500 μM benzyl alcohol. The staining was allowed to progress for 15 min without arresting the flow to avoid biofilm detachment of the *P. putida* strain. Using this relatively short staining time, *P. putida* cells were stained at a relatively low level compared to *Acinetobacter* cells.

Microscopy and image analysis of biofilms. All microscopic observations and image acquisitions were performed on a Zeiss LSM510 confocal laser scanning microscope (CSLM; Carl Zeiss, Jena, Germany) equipped with an argon-krypton laser and with detectors and filter sets for monitoring green fluorescent protein (GFP) and Syto62 and for the recording of reflection (light) images. Images were obtained using a 63×/1.4 Plan-APOChromat differential interference contrast objective or a 40×/1.3 Plan-Neofluor oil objective. Multichannel simulated fluorescence projection (SFP) images, vertical *xz* sections through the biofilms, and simulated three-dimensional (3D) images were generated by using the IMARIS software package (Bitplane). This software was used to remove the Syto62 signal from the GFP-fluorescent *P. putida* cells. Images were further processed for display by using Photoshop software (Adobe, Mountain View, CA).

Biofilm images of the mixed-species consortia were obtained to quantify biomass as described previously (23), using COMSTAT software. Twelve images from three independent biofilms were analyzed for each time point.

In order to quantify the degrees to which both the *P. putida* rough variant and the wt associated with the *Acinetobacter* microcolonies, specific 3D image algorithms were developed for calculating distributions of the distances from the surfaces of the *P. putida* cells to the surfaces of the *Acinetobacter* microcolonies/cells. In order to segment the biofilms from the background, the biofilm images of both *Acinetobacter* and *P. putida* were subjected to a threshold, using the Otsus method (40). In addition, morphological filtering (the so-called AreaOpen operation) was used to eliminate small colonies of background noise and interference noise between the channels. Additional image layers were then introduced by bilinear interpolation in order to obtain a voxel size with equidistant edges. Next, a 3D distance map defining the nearest distance from any voxel in the considered 3D mesh to the surfaces of *P. putida* cells was calculated by use of a previously described 3D Euclidean distance transform (60). The distance values belonging to voxels overlapping with the surface regions of the *Acinetobacter* biofilm were then collected to produce the distribution of distances between strains. A minimum of eight images from two independent biofilms were analyzed for each time point.

Oxygen upshift and downshift experiments. A method was developed to control the oxygen concentration in the inflowing biofilm medium. Due to the high oxygen permeability of the silicone tubing feeding the flow channel, it was possible to control the oxygen concentration in the inflowing medium. This was done by passing the medium through 5 m of silicone tubing submerged in a water container purged with either nitrogen gas (99.8% N_2; Hede Nielsen, Denmark) or oxygen gas (99.5%; Hede Nielsen, Denmark) prior to its entering the flow channel. Oxygen concentrations were measured using a microelectrode with a 0.5-mm tip (Unisense OX500) connected to an ampere meter with a built-in polarization source (Unisense PA2000). Before every set of measurements, a calibration curve was obtained by determining the value at zero oxygen (water vigorously purged with nitrogen gas) and the value for water saturated with air

(which corresponds to approximately 250 μM oxygen at 24°C and 0.9% NaCl [18]).

Oxygen downshift experiments (one step down) were performed on 2-day-old biofilms consisting of mixed-species *Acinetobacter* and *P. putida* populations or a monospecies *P. putida* population grown as described above. To monitor downshift experiments online using scanning confocal microscopy, the flow cell was connected to the submerged silicone tubing by a glass tube to prevent influx of oxygen. The biofilm populations were fed with air-saturated biofilm medium until the desired time point for the downshift, shifted to the oxygen-stripped medium at time zero, and subsequently followed over time. In order to efficiently strip the oxygen from the biofilm medium, the silicone tubing had been submerged in N_2-purged water additionally containing the reductant sodium ascorbate (0.1 M).

Oxygen upshift experiments were performed as described for the downshift experiments except that the water tank was purged with O_2 gas, which resulted in an oxygen concentration of around 1 mM in the medium inflow.

Stepwise downshift experiments were performed on *P. putida* monospecies biofilms formed by the wt or the rough variant, propagated as described above. After inoculation, the silicone tubing, including the flow cells, was submerged and secured in a 15-liter water-filled tank. The oxygen concentration in the inflow medium was monitored by measuring the concentration of oxygen in the water container, which in turn was controlled by the purging rate of nitrogen gas (control experiments had shown a <2% difference in the concentrations in the inflow medium and the water surrounding the silicone tubing, which was mainly due to a difference in the saline concentration). The oxygen concentration in the water was adjusted to obtain an oxygen concentration of approximately 125 μM (50% of the normal level). After 18 h of incubation, the concentration was reduced to approximately 100 μM (40%), and after 24 h, it was reduced to approximately 75 μM (30%). After 32 h, the oxygen concentration was reduced to 35 μM (14%) and, finally, to near zero levels (<3 μM). During the experiment, the flow cells were briefly removed from the water tank for microscopic observations and image acquisition (brief upshifts had no significant effect on the biofilms).

Phenotypic characterization of the *P. putida* rough variant. Swimming motility and chemotaxis (42) towards benzoate were investigated using 0.28% agar plates with AB medium supplemented with 1 mM benzoate (Sigma). Single colonies were inoculated, and plates were incubated for 24 h at 30°C.

P. putida wt and rough variant strains were investigated for pellicle formation in static broth cultures. A 100-ml Erlenmeyer flask containing 50 ml AB minimal medium supplemented with 40 mM glucose was inoculated with 1 ml overnight culture. Cultures were incubated without shaking at 30°C, and pellicle formation was observed after 2 days. The pellicle polysaccharide was stained with calcofluor white (Sigma) as described previously (36), except that the buffer (10 mM Tris buffer, pH 8, 0.9% NaCl) contained 1 μg/ml calcofluor white. The polysaccharide was examined using an Axioplan epifluorescence microscope (Carl Zeiss) with a 100× oil objective. The microscope was equipped with a 100-W mercury lamp and a DAPI (4′,6′-diamidino-2-phenylindole) filter. To confirm the presence of a cellulose-like polymer in the rough variant pellicle biofilm, pellicle material from static cultures was treated with cellulase (from *Aspergillus niger*; ICN Biomedicals Inc.) as described previously (51), with the addition of 5 μg/ml chloramphenicol to stop bacterial protein synthesis. Disintegration of pellicles was determined by visual inspection. Extracellular polysaccharide (EPS) formation in *P. putida* wt and variant colonies was examined on fresh LB agar plates with 25 μg/ml calcofluor white. Plates were incubated at 30°C for 5 days. The binding of calcofluor white to agar plate colonies was determined by fluorescence excitation with a 254-nm light source and photographed using a Canon digital camera.

Coaggregation of *Acinetobacter* and *P. putida* cells (GFP-tagged wt and rough variant cells) was investigated by mixing cells from stationary-phase cultures. The cell density (optical density at 600 nm) was adjusted to 1.5, and cells were subsequently mixed at a ratio of 1:1 in a total volume of 1 ml. Aggregation was allowed to proceed for 3 h before inspection. For microscopic visualization, cells were stained with 0.2% Syto62 for 30 min, and images were obtained using an LSM510 microscope as described above. Cellulase assays on coaggregated clumps were performed as described above for the rough variant pellicle biofilm material.

RESULTS

Biofilm development and in situ growth physiology. Biofilm development and structural coordination in mixed-species consortia of *Acinetobacter* sp. strain C6 and either *P. putida* wt KT2440 or the isolated rough variant were investigated by confocal microscopy in flow chambers irrigated with 500 μM of benzyl alcohol. Previous reports have shown that benzoate continuously leaks from the large *Acinetobacter* microcolonies (7, 37). *P. putida* KT2440 is totally dependent on the benzoate cross-feeding activity of *Acinetobacter* when the mixed-species consortium is propagated on benzyl alcohol, but despite the apparent advantage of associative behavior, it was obvious throughout the observed period of biofilm formation that the ancestral *P. putida* KT2440 strain was unable to enter close structural associations with *Acinetobacter* (Fig. 1A and B). Moreover, within 3 to 4 days, the *Acinetobacter* population became increasingly dominant in some areas (Fig. 1C). In contrast, the *P. putida* rough variant proliferated successfully in the presence of *Acinetobacter* while remaining tightly associated throughout the course of development (Fig. 1D and E). The *P. putida* wt biofilm structure was loose and protruding (no dense colonies), as previously described for *P. putida* OUS82 (54), with a flexible and elastic response to abrupt changes in flow velocity. In comparison, however, the rough variant developed a very inflexible biofilm structure. Rough variant cells covered almost the entire exposed surface of the *Acinetobacter* biofilm, and mixed microcolonies were regularly observed (Fig. 1F). The observed developments and dynamics of the wt and variant consortia were further supported by computer analysis of biofilm images, using COMSTAT software (26). Biomass quantification of the wt consortium thus revealed that the total *P. putida* wt population decreased from day 1 to day 3 while the *Acinetobacter* population nearly doubled (Fig. 1G and H). Quantification of the rough variant consortium demonstrated a successfully reproducing rough variant population with a previously described (23) exploitative (negative) effect on the *Acinetobacter* population, in contrast to the wt consortium (Fig. 1G and H). The associative patterns of the wt and variant consortia on day 1 and day 3 were analyzed using a novel COMSTAT extension (see Materials and Methods) that calculated the average distance (μm) from the surfaces of *Acinetobacter* microcolonies and cells to the nearest *P. putida* cells. These data showed that rough variant cells of *P. putida* were associated closely with *Acinetobacter* microcolonies, whereas the nearest *P. putida* wt cells, on average, were located at a short distance (Fig. 1I). The differences in biofilm behavior and productivity between *P. putida* wt and variant populations could not be explained by differences in the ability to proliferate on benzoate, as growth rates of shaken batch cultures could not be distinguished data not shown).

In order to understand the inability of the ancestral *P. putida* population to efficiently colonize *Acinetobacter* microcolonies, the development and dynamics of in situ growth activity in the mixed-species biofilm were investigated. The *P. putida* KT2440 wt strain used in this study had a growth activity monitor cassette with a gene encoding an unstable version of GFP downstream of a ribosomal promoter inserted into the chromosome. This unstable version of GFP has a half-life of about 1 h in *P. putida* cells (34). With this insertion, growing cells will appear fluorescent green, whereas nongrowing cells will quickly lose fluorescence due to degradation of GFP in cells with no net protein synthesis (52). This construct allowed online studies of the growth activity distribution of *P. putida* cells growing in the biofilm consortium. Microscopic investigations revealed both temporary and structure-related dynamic

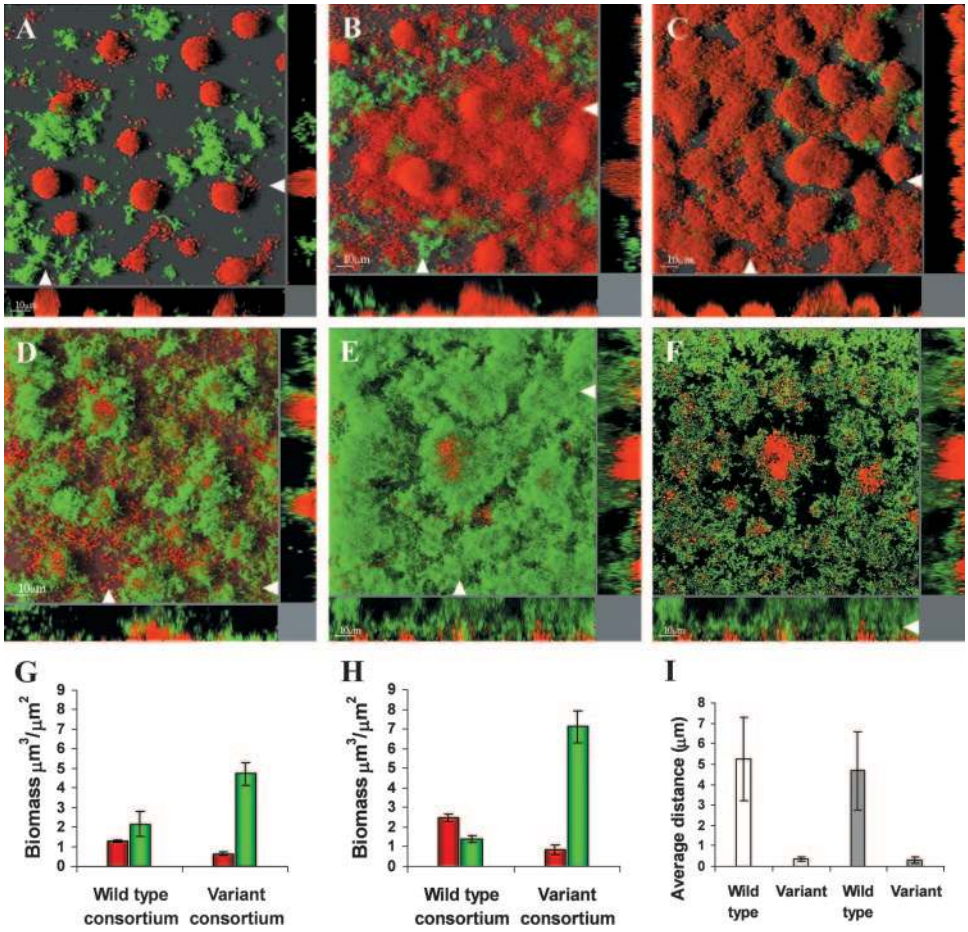

FIG. 1. Structural relationships and development of wt and evolved consortium biofilms. Biofilms of *Acinetobacter* sp. strain C6 and *P. putida* wt (A to C) or a *P. putida* rough variant (D to F) were grown in flow chambers supplemented with 500 μM benzyl alcohol as the sole carbon source. *P. putida* cells (green) had a *gfp* expression cassette inserted into the chromosome. *Acinetobacter* sp. strain C6 cells (red) were visualized using Syto62. CSLM micrographs were obtained for biofilms grown for 1 day (A and D) and 3 days (B, C, E, and F). The main frames (A to E) are horizontal shadow projection (SFP) images, and side panels are *xz* sections in the positions indicated with white arrows. The main frame in panel F is a single image slide from the image shown in panel E showing a high association between microcolonies of *Acinetobacter* and the *P. putida* rough variant. Biomass ($\mu m^3/\mu m^2$) distributions were determined on day 1 (G) and day 3 (H) by image quantification of biofilms consisting of the wt consortium (*P. putida* wt and *Acinetobacter*) and the variant consortium (*P. putida* rough variant and *Acinetobacter*), respectively. (Day 3 data were reproduced from *Nature* [23] with permission of the publisher.) Red, biomass of the *Acinetobacter* population; green, biomass of the *P. putida* population. Values are means ± standard deviations. (I) The structural association between *P. putida* and *Acinetobacter* was quantified by image analysis of the mixed-species biofilms (see Materials and Methods for details). The average distances from the surfaces of *Acinetobacter* microcolonies to the nearest *P. putida* cells were determined for the wt consortium and the rough variant consortium on day 1 (white bars) and on day 3 (gray bars). Values are means ± standard deviations.

changes in growth physiology. Although generally not associating with *Acinetobacter* microcolonies, the *P. putida* cells were fluorescent green, indicating active growth, throughout the first 24 to 36 h (data not shown). At this time, it was observed that very large *Acinetobacter* microcolonies seemed to exert a growth rate-decreasing activity in a gradient mode on *P. putida* cells situated at the substratum inside or in very close proximity to *Acinetobacter* microcolonies (Fig. 2). Gradually, within 48 h, the entire *P. putida* population had a significantly decreased growth activity (low GFP fluorescence), possibly caused by nutrient limitation. Aerobic degradation of aromatics requires molecular oxygen, and nutrient gradients are likely to appear due to the structured heterogeneous environment of the biofilm (5, 13, 57, 59). It was therefore considered possible that oxygen limitation could develop, which led us to investigate if oxygen limitations could explain part of the observed biofilm development and dynamics.

Investigation of oxygen limitations. The inflowing biofilm medium contained approximately 250 μM oxygen (medium saturated with air at 24°C) and 500 μM benzyl alcohol. To determine the oxygen consumption of biofilms, replicate mixed-species populations of *Acinetobacter* and *P. putida* wt were propagated in flow chambers, and the total oxygen consumption was measured. Measurements were obtained using an oxygen microelectrode with a 0.5-mm tip and a T-connector device applied to the system just before and after each flow channel, including a control without a biofilm population. The oxygen concentration dropped from approximately 250 μM in the influent biofilm medium to 8 μM ± 4 μM (mean ± standard deviation) on day 1 and <2 μM on day 2 in the effluent

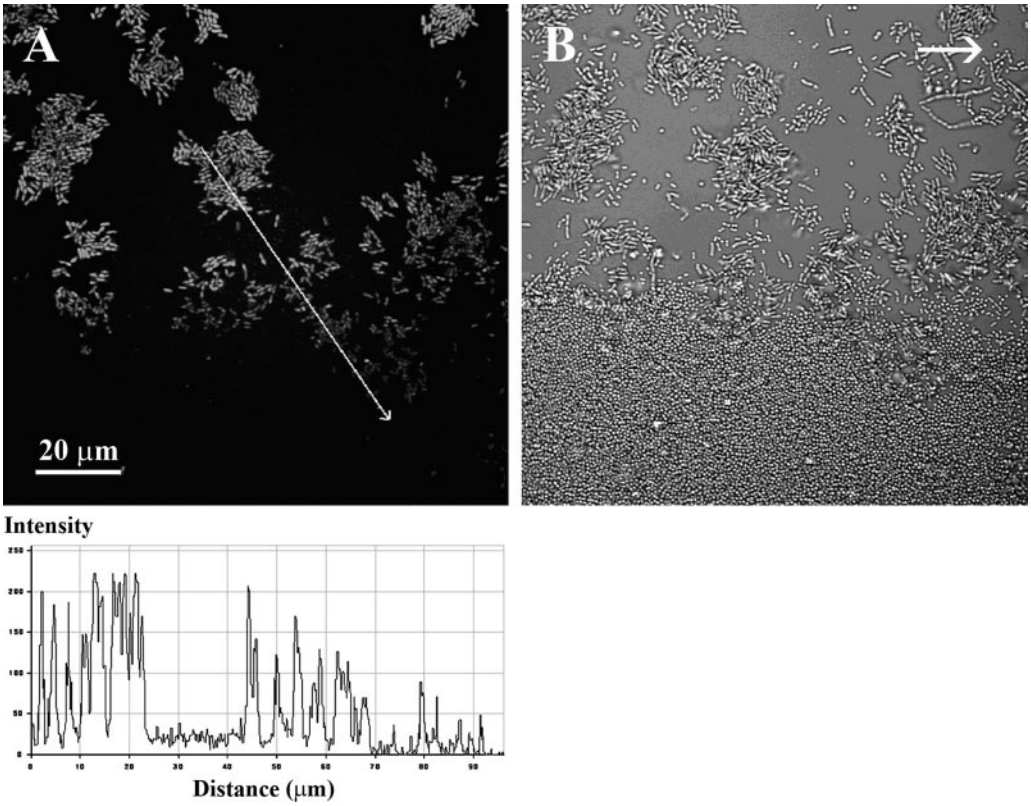

FIG. 2. Gradients in growth activity of *P. putida* cells at the bottom edge of large *Acinetobacter* sp. strain C6 microcolonies. To visualize in situ growth activity, the *P. putida* wt strain had a mini-Tn*7*–Gm^r–*rrnB*P1–*gfp*[AAV] cassette inserted into the chromosome. Mixed-species biofilms of *Acinetobacter* and *P. putida* were grown in flow chambers for 36 h. (A) Image of GFP fluorescence of *P. putida* cells (substratum layer) obtained using CSLM. The gradient in fluorescence intensity (bottom) was quantified along the line indicated with the white arrow. (B) Light reflection image captured in the same viewing field, showing both *P. putida* and *Acinetobacter* cells. The typical cell morphology of *Acinetobacter* is coccoid, and that of *P. putida* is rod-shaped, but the nonfluorescent rod-shaped cells in panel B are stressed or undivided cells of *Acinetobacter*, which are frequently seen for this strain when it is proliferated on a surface. The arrow in panel B shows the direction of flow.

medium, as determined for three independent experiments. It should be noted that the determined oxygen levels reflect the activities of both the resident biofilm population and the detached planktonic cells. The results thus showed a rapid decrease in total oxygen concentration, but this does not necessarily imply that oxygen became the limiting nutrient in situ in the mixed-species consortium. To this end, the mixed-species consortium with the *P. putida* wt strain harboring the growth activity reporter cassette was propagated. On day 2, when the general growth activity of the *P. putida* wt population was quite low, an oxygen upshift (see Materials and Methods) was performed by increasing the oxygen concentration in the inflowing medium from 250 μM to around 1 mM oxygen. Solely by raising the oxygen level, we found that the growth activity of *P. putida* was enhanced within 1 h following the upshift (Fig. 3). These results strongly suggest that oxygen did in fact become a limiting nutrient, and taken together with the high level of oxygen consumption, it is possible that the temporary and structural heterogeneity in growth activity observed for *P. putid*a was due to oxygen limitation. The growth rate-decreasing activity exerted by *Acinetobacter* on *P. putida* cells associated with the very large *Acinetobacter* microcolonies could thus simply be the result of oxygen limitation due to oxygen consumption by the *Acinetobacter* cells.

Biofilm dispersal in response to oxygen starvation. Biofilm dispersal in response to nutrient starvation has been reported for several biofilm populations (1, 14, 20, 53), and this phenomenon is recognized as an important part of surface colonization strategies (22). For *Pseudomonas putida* strain OUS82, biofilm dispersal in response to carbon starvation was demonstrated (20), and for *Shewanella oneidensis* biofilms, removal of oxygen resulted in biofilm detachment (53). These findings made us investigate if the ancestral *P. putida* KT2440 biofilm would detach in response to oxygen starvation and whether the *P. putida* rough variant would display a different biofilm dispersal response. In order to investigate this possibility, mixed populations of *Acinetobacter* sp. strain C6 and the *P. putida* wt strain or rough variant were propagated in flow chambers with benzyl alcohol as the sole carbon source. On day 2, an oxygen downshift was performed by decreasing the oxygen concentration in the inflowing biofilm medium from 250 μM to near zero levels (<2 μM). Biofilms were studied online using confocal microscopy and followed over time (Fig. 4). Within minutes, the first signs of biofilm detachment were observed for the *P. putida* wt strain (Fig. 4B), and the majority of the biofilm had detached after only 25 min (Fig. 4D). In contrast, the *P. putida* rough variant was unresponsive to the oxygen downshift in the consortium environment, and no bio-

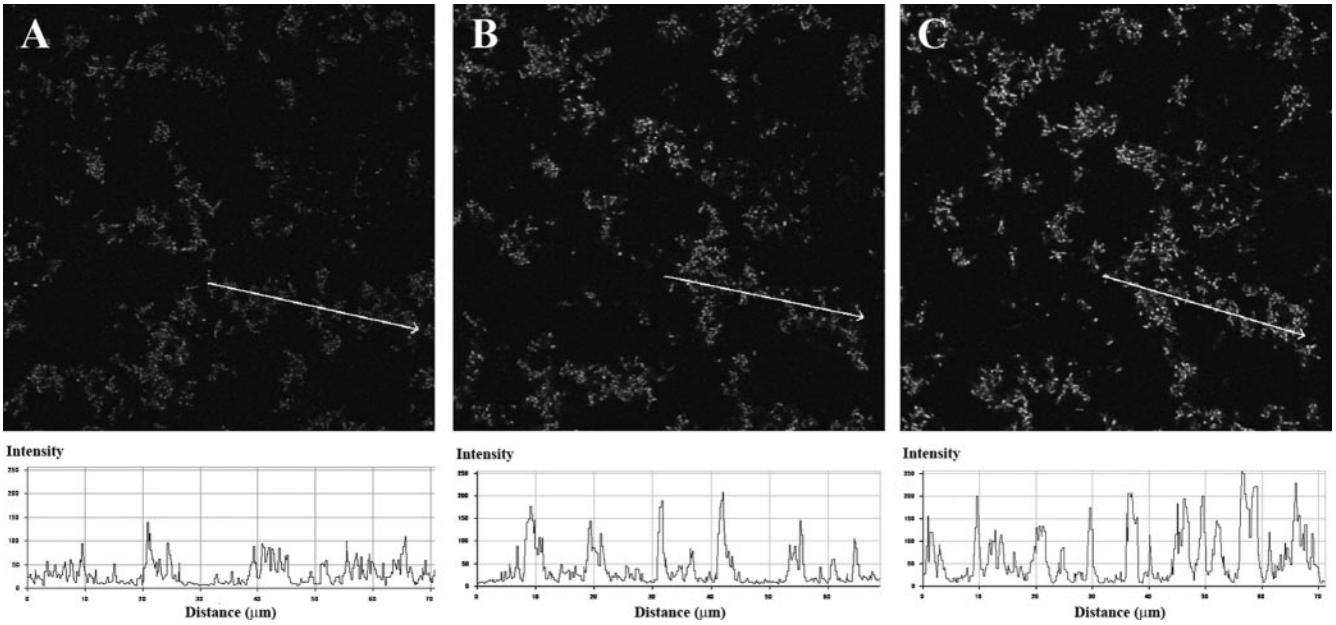

FIG. 3. Oxygen upshift causes increased growth activity of *P. putida* wt cells grown in mixed biofilms with *Acinetobacter* sp. strain C6 cells. *P. putida* wt cells containing a mini-Tn*7*–Gm^r–*rrnB*P1–*gfp*[AAV] cassette were grown in flow cells containing *Acinetobacter*. On day 2, the oxygen concentration in the inflowing medium was increased approximately fourfold, as described in Materials and Methods. CSLM micrographs of the GFP fluorescence were captured in the same viewing field before (A) and 30 min (B) and 60 min (C) after the oxygen upshift. Increased growth activity was observed in three independent experiments. Images were recorded as single horizontal scans. The gradient in fluorescence intensity shown below each image was quantified along the line indicated with the arrow, using LSM510 CSLM software. *Acinetobacter* cells are not visible.

film dispersal was observed (Fig. 4E and F), even after several hours of oxygen starvation. Investigations of two separately evolved, isolated rough variants showed that they also did not disperse the biofilm in response to an oxygen downshift (data not shown). Biofilm dispersal of the *P. putida* wt was not observed in response to carbon starvation in the consortium environment following 5 h of starvation (data not shown). These findings suggest that the inability of *P. putida* KT2440 to successfully compete in the mixed-species biofilm environment and to efficiently colonize *Acinetobacter* microcolonies may be due at least in part to the inherent biofilm dispersal in response to oxygen starvation. This suggestion is supported by the findings that the repeatedly selected rough variant efficiently colonized *Acinetobacter* microcolonies and, furthermore, showed

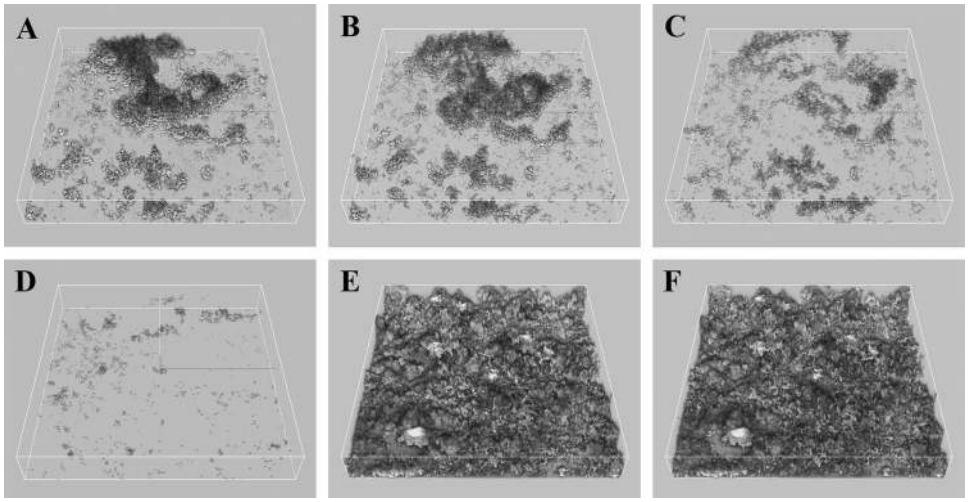

FIG. 4. Different biofilm dispersal phenotypes of *P. putida* wt and the rough variant in response to oxygen downshift. *Acinetobacter* cells were proliferated in flow chambers with GFP-tagged cells of *P. putida* wt and the rough variant. On day 2, an oxygen downshift was performed online as described in Materials and Methods. CSLM micrographs of the *P. putida* wt biofilm were captured in the same viewing field before (A) and 5 min (B), 9 min (C), and 25 min (D) after the oxygen downshift. CSLM micrographs of the *P. putida* rough variant biofilm were likewise captured in the same viewing field before (E) and 25 min after (F) the oxygen downshift. CSLM micrographs are presented as simulated three-dimensional images. *Acinetobacter* cells are not visible.

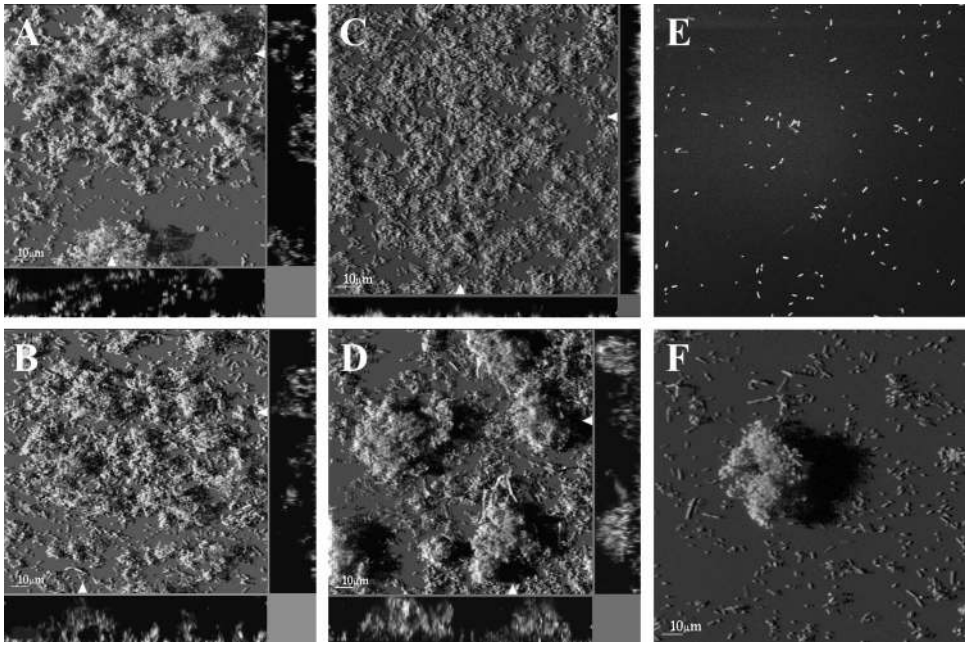

FIG. 5. Structures and phenotypes of *P. putida* wt and rough variant monospecies biofilms during a stepwise oxygen downshift. Biofilms were proliferated in flow chambers supplemented with benzoate as the sole carbon source. Green fluorescence from GFP-tagged *P. putida* cells was recorded using CSLM imaging. Monospecies biofilms of *P. putida* wt (A) and the rough variant (B) displayed a similar structure (day 2) when biofilms were proliferated with standard oxygen concentrations (approximately 250 μM in the inflowing medium). A graduated (stepwise) oxygen downshift was performed on monospecies biofilms as described in Materials and Methods. After 32 h, the inflowing medium contained approximately 75 μM oxygen, resulting in a very flat and thin biofilm of the *P. putida* wt population (C), in contrast to the thick microcolonies observed for the rough variant (D). After 48 h and prolonged starvation (down to <3 μM oxygen), both *P. putida* wt (E) and the rough variant (F) showed significant dispersal of the biofilm. The main frames are horizontal shadow projection (SFP) images, and side panels are *xz* sections in the positions indicated with white arrows.

a nondispersal biofilm phenotype in the consortium environment.

***P. putida* rough variant biofilm physiology.** In a further phenotypic characterization of the *P. putida* rough variant, the oxygen downshift experiment was carried out with monospecies biofilms (in the absence of *Acinetobacter*) of *P. putida* wt and the rough variant. Biofilm populations were propagated on 200 μM benzoate (since *P. putida* does not grow on benzyl alcohol) and followed microscopically for 2 days before the oxygen downshift was performed. Both strains showed a complete dispersal response to oxygen starvation (data not shown). In fact, the *P. putida* rough variant displayed a biofilm structure very similar to the loose and protruding structure of the wt biofilm described above (Fig. 5A and B). The addition of benzyl alcohol, in addition to benzoate, to the inflowing biofilm medium did not significantly influence the biofilm formation of the two strains (data not shown).

In an attempt to imitate the oxygen concentration dynamics in the mixed-species consortium, the oxygen downshift experiment was modified to gradually decrease the oxygen concentration in the inflowing biofilm medium. Monospecies populations of *P. putida* wt and the rough variant were inoculated in flow chambers irrigated with 1 mM benzoate, after which the oxygen concentration was gradually decreased (stepwise) over a 2-day period. Microscopic observations showed (after 32 h) that the *P. putida* rough variant population formed thick microcolonies in a biofilm medium containing around 30% of the normal oxygen level (approximately 75 μM), in contrast to the rather flat, thin wt biofilm (Fig. 5C and D). However, under conditions of prolonged starvation (48 h), both the wt and variant populations significantly dispersed the biofilm (Fig. 5E and F). These results show that although the *P. putida* rough variant displayed a transient improvement in biofilm persistence, conditions of decreased oxygen concentrations alone (absence of both benzyl alcohol and *Acinetobacter*) did not give rise to the nondispersal, low-oxygen-persistence phenotype.

These data show that the low-oxygen-persistence physiology of the rough variant is not expressed under all conditions. Since the rough variants evolved specifically in the presence of *Acinetobacter* sp. strain C6, we investigated if the sole presence of *Acinetobacter* cells in the flow chamber with the rough variant would cause the nondispersal, low-oxygen-persistence phenotype of the variant independent of the nutrient conditions. This was done by proliferating populations of the rough variant and *Acinetobacter* in the flow chamber on benzoate instead of benzyl alcohol. Flow chambers were supplied with standard air-saturated medium inflow. In this scenario, both strains were competing for the primary carbon source, and hence there was no apparent advantage for the rough variant to associate with *Acinetobacter* sp. strain C6. Not surprisingly, a large part of the rough variant population was found dissociated from the *Acinetobacter* microcolonies, and this part dispersed after the oxygen downshift, as observed for the *P. putida* wt population (data not shown). However, the part that was found associated with *Acinetobacter* microcolonies showed the characteristic nondispersal phenotype, indicating that proliferation associ-

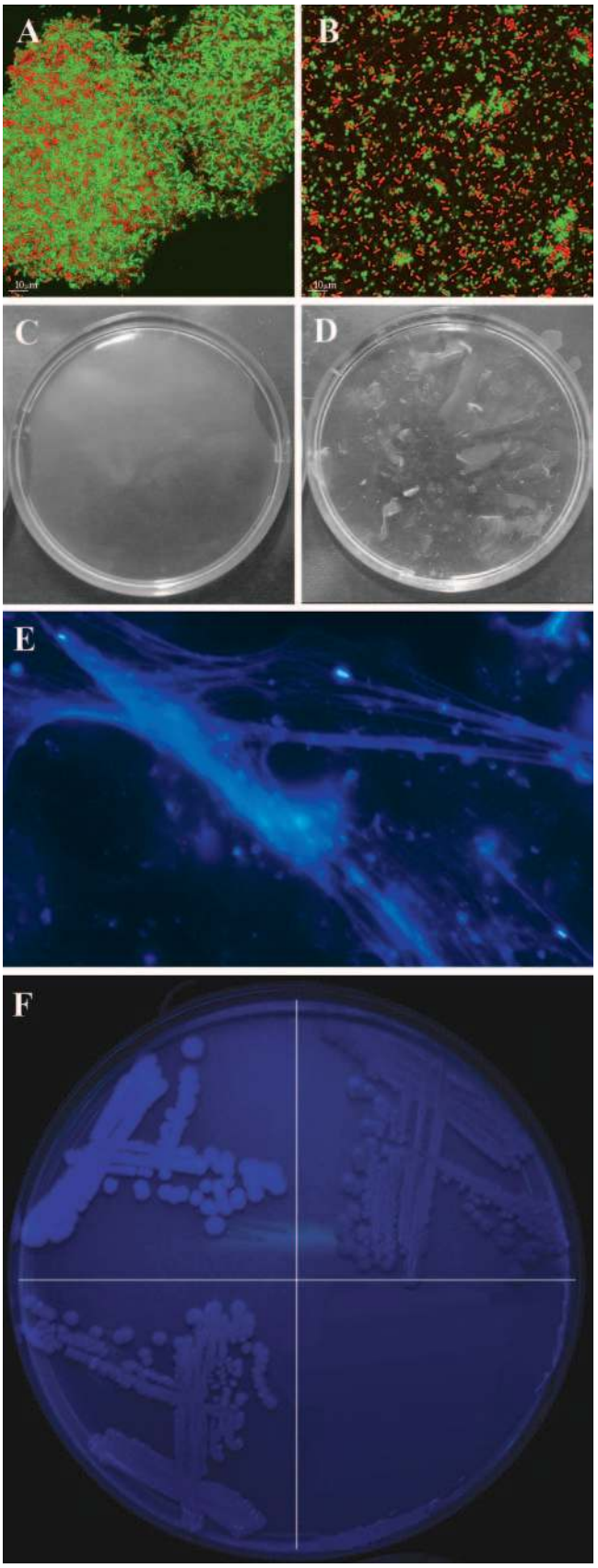

ated with *Acinetobacter* microcolonies may change the rough variant phenotype.

Coaggregate formation. The *P. putida* rough variant lacks the LPS O antigen as a consequence of the *wapH* mutation, which is very likely to change the physiochemical characteristics of the cell surface (47). This led us to investigate if the mutation had caused a change in surface compatibility between the rough variant and *Acinetobacter* cells, leading to increased coadhesion. Stationary-phase cultures were mixed at a ratio of 1:1 and allowed to aggregate for 3 h. At this time, coaggregation of *Acinetobacter* and *P. putida* rough variant cells formed large visible clumps in the mixture (Fig. 6A), whereas no significant clumping was observed for the mixture of *Acinetobacter* and *P. putida* wt (Fig. 6B). Rough variant cells grown on FAB minimal medium containing benzoate coaggregated into visual clumps with *Acinetobacter* cells grown in FAB medium containing benzyl alcohol; however, larger clumps formed at a higher rate when the rough variant was mixed with *Acinetobacter* cells grown in LB medium.

EPS formation in *P. putida* rough variants. The *P. putida* rough variant used in this study has a mutation in *wapH* (PP4943), a *P. aeruginosa* PAO1 *wapH* homolog (33, 35) involved in outer core LPS formation, conferring the rough colony morphology and cell shape (23). The conditionally inflexible biofilm structure observed for the variant suggested that cell surface properties and/or extracellular matrix materials were involved in changing the biofilm structure. Rough or wrinkled colony variants of other bacteria have previously been found to overproduce cellulose or cellulose-like polymers, making them capable of forming a pellicle in standing cultures (48, 50, 61). Interestingly, we found that the derived rough variant, but not the wt, was able to produce an elastic gel-like pellicle in standing broth cultures containing LB broth or glucose minimal medium (Fig. 6D). The pellicle was visible from day 2, progressively thickening over the following days. Epifluorescence microscopy of condensed pellicle material showed that the variant EPS material bound calcofluor white, an indicator of cellulose(-like) polymers that specifically binds to (1-3)- and (1-4)-β-D-glucopyranosyl units (Fig. 6E). In order to test if the robustness of the biofilm was secured by the calcofluor white-binding exopolysaccharide, standing broth cultures

FIG. 6. Coaggregation with *Acinetobacter*, biofilm pellicle formation, and polysaccharide formation observed for the *P. putida* rough variant are caused by the *wapH* mutation. (A and B) A stationary-phase cell culture of *P. putida* (green) grown on FAB medium with 5 mM benzoate was mixed with a stationary-phase cell culture of *Acinetobacter* sp. strain C6 (red) grown on LB. CSLM micrographs were obtained of coaggregates of *Acinetobacter* and *P. putida* rough variant cells (A) or *Acinetobacter* and *P. putida* wt cells (B) after 3 h of incubation. (C and D) Rough variant biofilm pellicles were transferred to a petri dish and incubated at 37°C overnight in the presence (C) and absence (D) of cellulase enzyme (from *Aspergillus niger*), as described in Materials and Methods. Dissolution was observed only after incubation with the cellulase enzyme. (E) Polysaccharide fibers of condensed biofilm pellicle material stained with calcofluor white. (F) Colonies of *P. putida* with a constructed mutation in the *wapH* gene (SNZ83) (top left), *P. putida* KT2440 wt (top right), and *P. putida* (SNZ83) complemented with a plasmid containing the *wapH* gene (bottom right) were grown on LB agar containing 25 μg/ml calcofluor white for 5 days.

of the rough variant were incubated for 5 days, after which the pellicles were treated with cellulase enzyme. After overnight incubation at 37°C, the treated pellicles had disintegrated (Fig. 6C), whereas untreated pellicles remained intact (Fig. 6D). To compare cellulose(-like) production in the wt versus variant strains and to determine if the *wapH* mutation alone was causing the polysaccharide production, we used the untagged *P. putida* KT2440 wt strain and a constructed rough variant thereof (SNZ83) (see reference 23 for construction details) with an introduced nonpolar mutation in the *wapH* gene. Pellicle formation was also observed in SNZ83. Colonies grown on agar plates containing the calcofluor white stain clearly showed an enhanced production of the cellulose-like polymer in the constructed rough variant (Fig. 6F, top left quadrant). Additionally, the calcofluor white-stainable material was not expressed in *P. putida* wt at any recordable levels, in accordance with previous findings (55) (Fig. 6F, top right quadrant). The level of calcofluor white staining in *P. putida* SNZ83 harboring the *wapH* gene on plasmid pBBR4943-1 (23) was similar to the wt level, suggesting that production of the exopolysaccharide is a direct consequence of the mutation in *wapH* (Fig. 6F, bottom left quadrant).

In order to investigate the role of cellulose production in stabilizing the coaggregates of *Acinetobacter* and *P. putida* rough variant cells, aggregates were treated with cellulase as described for the pellicle biofilm (see above). However, no signs of dissolution were observed after overnight incubation (data not shown). Attempts to dissolve the mixed-species biofilm of *Acinetobacter* and the *P. putida* rough variant with cellulase treatment also failed (data not shown).

DISCUSSION

When *P. putida* KT2440 and *Acinetobacter* sp. strain C6 are propagated in mixed-species biofilms on benzyl alcohol, the *P. putida* population is totally dependent on benzoate cross-feeding from *Acinetobacter* cells. In the course of biofilm development, the reproducible appearance of better-adapted rough colony morphology variants of *P. putida* was observed as described previously (23). The rough variant formed tight structural associations with the *Acinetobacter* population and efficiently colonized the *Acinetobacter* biofilm surface, which was confirmed by image analysis. The ability to interact structurally is very likely part of the selective advantage of this variant due to the dependence on cross-fed benzoate. In contrast, the *P. putida* wt strain clearly lacked the capacity to form such tight structural associations with *Acinetobacter* microcolonies and to persist successfully over time. These observations raise the question of which specific phenotypic properties are needed for the completely changed persistence phenotype of *P. putida* KT2440.

One possible explanation for the observed phenotypic differences could be a change in chemotactic behavior, given that *P. putida* is chemotactic towards benzoate, the cross-fed substrate (24, 25). Chemotaxis and motility have been shown to be very important for biofilm structure and coordination in surface populations (28, 29, 39). Our own investigations have documented that both *P. putida* wt and rough variant cells are motile and show a positive chemotactic response to increasing concentrations of benzoate (data not shown). Despite a small reduction in swimming speed of the rough variant, the differences in motility behavior cannot explain the observed difference in structural association in the mixed-species biofilms.

The *P. putida* wt population was unable to establish a tight association with the *Acinetobacter* microcolonies, and furthermore, a decline in population size was observed over time. The underlying theory behind this failure involves the oxygen starvation response. It is hypothesized that as they are confronted with reductions in oxygen levels, *P. putida* cells respond by leaving the biofilm rather than taking up competition for oxygen. The exact molecular basis for biofilm dispersal in *P. putida* KT2440 is unknown, but in *P. putida* OUS82, proteins containing the GGDEF and EAL domains have been shown to be involved in biofilm formation and dispersal (21). The biofilm dispersal mechanism was observed for *P. putida* wt biofilms in response to both a rapid and a more gradual oxygen downshift. The findings that the *P. putida* wt biomass decreased from day 1 to day 3, that the total oxygen consumption reached almost exhaustive levels within 1 to 2 days, that the growth activity of wt *P. putida* decreased first locally around large *Acinetobacter* microcolonies (Fig. 2) and then globally within 2 days, and that the growth rate-limiting nutrient at this point was in fact oxygen are all in accordance with our hypothesis. Benzoate limitation was unlikely to be the cause of the local growth activity decrease observed, because previous investigations have shown that benzoate is continuously leaking from the large microcolonies (37) and accumulating in the effluent medium (7) under similar conditions. Upshifting the oxygen concentration increased the growth activity of *P. putida* cells, showing that there was no lack of carbon source under the prevailing conditions (Fig. 3). Also, we found that benzoate was not toxic to *P. putida* at relevant concentrations (data not shown). Since the *P. putida* wt population disperses in response to oxygen starvation, a niche is open to any new variant that would be able to overcome this problem.

A complete change in dispersal response was observed for the *P. putida* rough variant: when mixed-species biofilms of the rough variant and *Acinetobacter* sp. strain C6 were exposed to low-oxygen conditions, no dispersal of the variant population was observed. Explaining the lack of an oxygen starvation response of the rough variant genotype in the mixed-species biofilms is complicated by the finding that these cells in fact do possess the normal biofilm dispersal response if confronted with a sudden depletion of oxygen in the absence of *Acinetobacter*, so the rough variant is not merely a biofilm dispersal mutant. In addition to the normal dispersal response observed for *P. putida* rough variant monospecies biofilms was the finding of loose and flexible biofilm structures similar to those observed for the wt. Hence, the rough variant flow chamber population displayed behavioral and structural similarity with the wt population in the absence of *Acinetobacter* cells, in support of our previous results (23) showing that rough variants did not evolve in monospecies biofilms of *P. putida* wt and that the rough variants did not have any fitness advantage relative to the ancestral *P. putida* cells in this environment.

One of the real challenges in this investigation was to explain how a single mutation resulting in a changed LPS phenotype gives rise to the observed conditional nondispersal phenotype. We therefore investigated various factors in the mixed-species biofilm environment in an attempt to resolve the specific con-

ditions leading to the characteristic conditional phenotype of the *P. putida* rough variant. As discussed above, it was clear that the presence of the *Acinetobacter* population in the biofilm was needed for the nondispersal phenotype to occur. One effect of the *Acinetobacter* population in the mixed-species biofilms was a gradual reduction in oxygen concentration due to extensive oxygen consumption from metabolizing the carbon source, benzyl alcohol. However, reduced oxygen conditions alone did not produce the complete nondispersal phenotype, as a gradual reduction in the externally applied oxygen concentration resulted in a transiently thicker monospecies biofilm of the rough variant compared to that of the wt, and prolonged starvation caused both strains to disperse significantly.

The lack of the O antigen in the rough variant is very likely to change the physiochemical characteristics of the cell surface (47), which could have a direct effect on the cell-to-cell interaction with *Acinetobacter* cells by changing the surface compatibility. It was previously shown that core or rough LPS variant derivatives of *P. aeruginosa* were more hydrophobic and showed changed biofilm-forming properties (16, 47). Experiments with batch cultures revealed that cells of *Acinetobacter* and the *P. putida* rough variant, but not wt *P. putida*, form extensive coaggregates when mixed together. The mechanism of coadherence is unknown, but this feature seems to be a key factor in understanding the conditional behavior of the rough variant: it is able to stick firmly and specifically to the *Acinetobacter* microcolonies or cells in the mixed-species biofilms and thereby ensure close access to the excreted benzoate. In this way, the *Acinetobacter* population may function as an anchor point for the rough variant, an opportunity not present in monospecies biofilms. However, just serving as an anchor point was not sufficient for the *Acinetobacter* population to cause the complete nondispersal phenotype of the rough variant population. This was demonstrated by propagating the mixed-species rough variant biofilm on a different nutrient source, i.e., benzoate, instead of benzyl alcohol. The part of the rough variant population that was found associated with *Acinetobacter* microcolonies when propagated on benzoate showed the characteristic nondispersal phenotype. However, other niches contained rough variant microcolonies with a phenotype similar to that of the wt; these microcolonies would detach when the oxygen concentration was shifted down. This suggests that proliferating in the environment in tight association with *Acinetobacter* microcolonies could change the rough variant physiology, although this was neither advantageous nor necessary under conditions where both strains were able to degrade the primary carbon source, benzoate.

We have previously shown that the rough variant has a parasitic or negative effect on the *Acinetobacter* population when they proliferate together in mixed-species biofilms (23). The results from this work point to intense oxygen competition in the biofilm environment, which offers a plausible explanation for the parasitic effect, as follows: the rough variant grows as a mantle on the *Acinetobacter* microcolonies (Fig. 1) and therefore acts as a living shield by preventing *Acinetobacter* cells from efficiently reaching the important nutrient oxygen. In the wt situation, the *P. putida* population responds by leaving when competition for oxygen becomes too intense.

We have shown that both benzyl alcohol and the *Acinetobacter* population are necessary but that neither one is sufficient for the complete nondispersal phenotype of the rough variant to occur. *Acinetobacter* cells may serve as an attachment point for the *P. putida* rough variant cells, but other adherence factors or matrix components seem to be needed to stabilize the variant biofilm, as not all variant cells can be attached directly to the *Acinetobacter* cells. It is very likely that growing in the stressful environment of the *Acinetobacter* microcolonies may induce the rough variant population to produce some extracellular polymeric substances. Some of the stress factors could be the very low concentration of oxygen, surface contact with *Acinetobacter* cells, or the generally poor nutrient environment. It is highly possible that the cellulose-like polymer that has been observed in the rough variant could be induced in the mixed-species biofilm and may be responsible, to some degree, for the nondispersal phenotype. However, it is clear that the cellulose-like polymer was not the only factor causing the nondispersal biofilm phenotype, as cellulase enzyme treatment of mixed-species biofilms with *Acinetobacter* did not disintegrate the biofilm.

Evidence of enhanced formation of a cellulose-like polymer in the rough variant was found on agar plates and in standing broth cultures producing a biofilm pellicle that could be disintegrated by cellulase enzyme treatment. Sequence analysis has revealed a cellulose operon in the *P. putida* genome (15, 38), and the EPS material could therefore be cellulose. In agreement with our results, no pellicle formation was observed for *P. putida* KT2440 wt in standing cultures of KB medium, but interestingly, the cellulose machinery was demonstrated to be intact and functioning (55). Additionally, cellulose production seems to be fairly common among bacteria and pseudomonads in relation to biofilm formation (55). The enhanced production of the cellulose-like polymer was shown to be the result of one mutation in *wapH*, a gene involved in core LPS production. The link between the mutation and the enhanced EPS production in *P. putida* is not clear, but a similar phenotype was found for the root-colonizing bacterium *Azospirillum brasilense*. In this case, a deletion causing a modification in the LPS core structure resulted in enhanced production of a calcofluor white-stainable polysaccharide (27). Deep rough LPS variant phenotypes of *Escherichia coli* have been shown to overproduce colanic acid EPS. These mutants are unable to cross-link the LPS core part (43), but the homologous genes involved in inner core LPS formation in *P. aeruginosa* were shown to be essential (56).

Our investigations show that biofilms may readily develop into very complex and heterogeneous environments, with structural niches, microenvironments, and gradients of nutrients, a finding that is consistent with the prevailing view of the biofilm environment (2). Nutrient (or oxygen) starvation causes subpopulation stress (3). The rapid and repeated emergence of rough colony variants is the result of natural selection (23) in response to the physical/chemical environment afforded by the presence of benzyl alcohol-degrading *Acinetobacter* cells; the shortcomings of the wt genotype are quickly overcome by adaptive mutations. The present results confirm our previous suggestion (23) that the rough variant phenotype is adapted to the very specific environment from which it was derived, and there is no reason to assume that the mutation has any selective advantage under other environmental conditions.

The specific adaptation could be caused by one single mutation in *wapH* altering entirely the interspecies interaction, biofilm structure, and phenotype, causing coaggregation and polysaccharide formation.

ACKNOWLEDGMENT

Support from the Danish Research Councils to S.M. is gratefully acknowledged.

REFERENCES

1. **Allison, D. G., B. Ruiz, C. SanJose, A. Jaspe, and P. Gilbert.** 1998. Extracellular products as mediators of the formation and detachment of Pseudomonas fluorescens biofilms. FEMS Microbiol. Lett. **167:**179–184.
2. **Beloin, C., and J. M. Ghigo.** 2005. Finding gene-expression patterns in bacterial biofilms. Trends Microbiol. **13:**16–19.
3. **Beloin, C., J. Valle, P. Latour-Lambert, P. Faure, M. Kzreminski, D. Balestrino, J. A. Haagensen, S. Molin, G. Prensier, B. Arbeille, and J. M. Ghigo.** 2004. Global impact of mature biofilm lifestyle on Escherichia coli K-12 gene expression. Mol. Microbiol. **51:**659–674.
4. **Boles, B. R., M. Thoendel, and P. K. Singh.** 2004. Self-generated diversity produces "insurance effects" in biofilm communities. Proc. Natl. Acad. Sci. USA **101:**16630–16635.
5. **Borriello, G., E. Werner, F. Roe, A. M. Kim, G. D. Ehrlich, and P. S. Stewart.** 2004. Oxygen limitation contributes to antibiotic tolerance of *Pseudomonas aeruginosa* in biofilms. Antimicrob. Agents Chemother. **48:**2659–2664.
6. **Caldwell, D., G. M. Wolfaardt, D. R. Korber, and J. R. Lawrence.** 1997. Do bacterial communities transcend Darwinism? Adv. Microb. Ecol. **15:**105–191.
7. **Christensen, B. B., J. A. Haagensen, A. Heydorn, and S. Molin.** 2002. Metabolic commensalism and competition in a two-species microbial consortium. Appl. Environ. Microbiol. **68:**2495–2502.
8. **Christensen, B. B., C. Sternberg, J. B. Andersen, R. J. Palmer, A. T. Nielsen, M. Givskov, and S. Molin.** 1999. Molecular tools for study of biofilm physiology. Methods Enzymol. **310:**20–42.
9. **Cisar, J. O., S. H. Curl, P. E. Kolenbrander, and A. E. Vatter.** 1983. Specific absence of type 2 fimbriae on a coaggregation-defective mutant of *Actinomyces viscosus* T14V. Infect. Immun. **40:**759–765.
10. **Cisar, J. O., A. L. Sandberg, G. P. Reddy, C. Abeygunawardana, and C. A. Bush.** 1997. Structural and antigenic types of cell wall polysaccharides from viridans group streptococci with receptors for oral actinomyces and streptococcal lectins. Infect. Immun. **65:**5035–5041.
11. **Clark, J. D., and O. Maaløe.** 1967. DNA replication and the cell cycle in *Escherichia coli* cells. J. Mol. Biol. **23:**293–300.
12. **Costerton, J. W., Z. Lewandowski, D. E. Caldwell, D. R. Korber, and H. M. Lappin-Scott.** 1995. Microbial biofilms. Annu. Rev. Microbiol. **49:**711–745.
13. **DeBeer, D., P. Stoodley, F. Roe, and Z. Lewandowski.** 1994. Effects of biofilm structures on oxygen distribution and mass-transport. Biotechnol. Bioeng. **43:**1131–1138.
14. **Delaquis, P. J., D. E. Caldwell, J. R. Lawrence, and A. R. McCurdy.** 1989. Detachment of Pseudomonas fluorescens from biofilm on glass surfaces in response to nutrient stress. Microb. Ecol. **18:**199–210.
15. **Dos Santos, V. A., S. Heim, E. R. Moore, M. Stratz, and K. N. Timmis.** 2004. Insights into the genomic basis of niche specificity of Pseudomonas putida KT2440. Environ. Microbiol. **6:**1264–1286.
16. **Flemming, C. A., R. J. Palmer, A. A. Arrage, H. C. Van de Mei, and D. C. White.** 1998. Cell surface physicochemistry alters biofilm development of Pseudomonas aeruginosa lipopolysaccharide mutants. Biofouling **13:**213–231.
17. **Franklin, F. C., M. Bagdasarian, M. M. Bagdasarian, and K. N. Timmis.** 1981. Molecular and functional analysis of the TOL plasmid pWWO from Pseudomonas putida and cloning of genes for the entire regulated aromatic ring meta cleavage pathway. Proc. Natl. Acad. Sci. USA **78:**7458–7462.
18. **Garcia, H. E., and L. I. Gordon.** 1992. Oxygen solubility in seawater: better fitting equations. Limnol. Oceanogr. **37:**1307–1312.
19. **Gieseke, A., L. Bjerrum, M. Wagner, and R. Amann.** 2003. Structure and activity of multiple nitrifying bacterial populations co-existing in a biofilm. Environ. Microbiol. **5:**355–369.
20. **Gjermansen, M., P. Ragas, C. Sternberg, S. Molin, and T. Tolker-Nielsen.** 2005. Characterization of starvation-induced dispersion in Pseudomonas putida biofilms. Environ. Microbiol. **7:**894–906.
21. **Gjermansen, M., P. Ragas, and T. Tolker-Nielsen.** 2006. Proteins with GGDEF and EAL domains regulate Pseudomonas putida biofilm formation and dispersal. FEMS Microbiol. Lett. **265:**215–224.
22. **Hall-Stoodley, L., and P. Stoodley.** 2005. Biofilm formation and dispersal and the transmission of human pathogens. Trends Microbiol. **13:**7–10.
23. **Hansen, S. K., P. B. Rainey, J. A. Haagensen, and S. Molin.** 2007. Evolution of species interactions in a biofilm community. Nature **445:**533–536.
24. **Harwood, C. S., and L. N. Ornston.** 1984. TOL plasmid can prevent induction of chemotactic responses to aromatic acids. J. Bacteriol. **160:**797–800.
25. **Harwood, C. S., M. Rivelli, and L. N. Ornston.** 1984. Aromatic acids are chemoattractants for *Pseudomonas putida*. J. Bacteriol. **160:**622–628.
26. **Heydorn, A., A. T. Nielsen, M. Hentzer, C. Sternberg, M. Givskov, B. K. Ersboll, and S. Molin.** 2000. Quantification of biofilm structures by the novel computer program COMSTAT. Microbiology **146:**2395–2407.
27. **Jofre, E., A. Lagares, and G. Mori.** 2004. Disruption of dTDP-rhamnose biosynthesis modifies lipopolysaccharide core, exopolysaccharide production, and root colonization in Azospirillum brasilense. FEMS Microbiol. Lett. **231:**267–275.
28. **Klausen, M., A. Aaes-Jorgensen, S. Molin, and T. Tolker-Nielsen.** 2003. Involvement of bacterial migration in the development of complex multicellular structures in Pseudomonas aeruginosa biofilms. Mol. Microbiol. **50:**61–68.
29. **Klausen, M., A. Heydorn, P. Ragas, L. Lambertsen, A. Aaes-Jorgensen, S. Molin, and T. Tolker-Nielsen.** 2003. Biofilm formation by Pseudomonas aeruginosa wild type, flagella and type IV pili mutants. Mol. Microbiol. **48:**1511–1524.
30. **Kolenbrander, P. E.** 2000. Oral microbial communities: biofilms, interactions, and genetic systems. Annu. Rev. Microbiol. **54:**413–437.
31. **Kolenbrander, P. E., P. G. Egland, P. I. Diaz, and R. J. Palmer, Jr.** 2005. Genome-genome interactions: bacterial communities in initial dental plaque. Trends Microbiol. **13:**11–15.
32. **Komlos, J., A. B. Cunningham, A. K. Camper, and R. R. Sharp.** 2005. Interaction of Klebsiella oxytoca and Burkholderia cepacia in dual-species batch cultures and biofilms as a function of growth rate and substrate concentration. Microb. Ecol. **49:**114–125.
33. **Lam, J. S., M. Matewish, and K. K. H. Poon.** 2004. Lipopolysaccharides of *Pseudomonas aeruginosa*, p. 3–51. *In* J. Ramos (ed.), Pseudomonas, vol. 3. Kluwer Academic/Plenum Publishers, New York, NY.
34. **Lambertsen, L., C. Sternberg, and S. Molin.** 2004. Mini-Tn7 transposons for site-specific tagging of bacteria with fluorescent proteins. Environ. Microbiol. **6:**726–732.
35. **Matewish, J. M.** 2004. The functional role of lipopolysaccharide in the cell envelope and surface proteins of *Pseudomonas aeruginosa*. Ph.D. thesis. University of Guelph, Guelph, Ontario, Canada.
36. **Matthysse, A. G., K. V. Holmes, and R. H. Gurlitz.** 1981. Elaboration of cellulose fibrils by *Agrobacterium tumefaciens* during attachment to carrot cells. J. Bacteriol. **145:**583–595.
37. **Møller, S., C. Sternberg, J. B. Andersen, B. B. Christensen, J. L. Ramos, M. Givskov, and S. Molin.** 1998. In situ gene expression in mixed-culture biofilms: evidence of metabolic interactions between community members. Appl. Environ. Microbiol. **64:**721–732.
38. **Nelson, K. E., C. Weinel, I. T. Paulsen, R. J. Dodson, H. Hilbert, V. A. Martins dos Santos, D. E. Fouts, S. R. Gill, M. Pop, M. Holmes, L. Brinkac, M. Beanan, R. T. DeBoy, S. Daugherty, J. Kolonay, R. Madupu, W. Nelson, O. White, J. Peterson, H. Khouri, I. Hance, L. P. Chris, E. Holtzapple, D. Scanlan, K. Tran, A. Moazzez, T. Utterback, M. Rizzo, K. Lee, D. Kosack, D. Moestl, H. Wedler, J. Lauber, D. Stjepandic, J. Hoheisel, M. Straetz, S. Heim, C. Kiewitz, J. A. Eisen, K. N. Timmis, A. Dusterhoft, B. Tummler, and C. M. Fraser.** 2002. Complete genome sequence and comparative analysis of the metabolically versatile Pseudomonas putida KT2440. Environ. Microbiol. **4:**799–808.
39. **Nielsen, A. T., T. Tolker-Nielsen, K. B. Barken, and S. Molin.** 2000. Role of commensal relationships on the spatial structure of a surface-attached microbial consortium. Environ. Microbiol. **2:**59–68.
40. **Otsu, A.** 1979. Threshold selection method from gray level histograms. Trans. Syst. Man Cybernet. **9:**62–66.
41. **Palmer, R. J., Jr., S. M. Gordon, J. O. Cisar, and P. E. Kolenbrander.** 2003. Coaggregation-mediated interactions of streptococci and actinomyces detected in initial human dental plaque. J. Bacteriol. **185:**3400–3409.
42. **Parales, R. E.** 2004. Nitrobenzoates and aminobenzoates are chemoattractants for *Pseudomonas* strains. Appl. Environ. Microbiol. **70:**285–292.
43. **Parker, C. T., A. W. Kloser, C. A. Schnaitman, M. A. Stein, S. Gottesman, and B. W. Gibson.** 1992. Role of the *rfaG* and *rfaP* genes in determining the lipopolysaccharide core structure and cell surface properties of *Escherichia coli* K-12. J. Bacteriol. **174:**2525–2538.
44. **Raetz, C. R. H.** 1996. Bacterial lipopolysaccharides: a remarkable family of bioactive macroamphiphiles, p. 1035–1063. *In* F. C. Neidhardt, R. Curtiss III, J. L. Ingraham, E. C. C. Lin, K. B. Low, B. Magasanik, W. S. Reznikoff, M. Riley, M. Schaechter, and H. E. Umbarger (ed.), *Escherichia coli* and *Salmonella*: cellular and molecular biology, vol. 1. ASM Press, Washington, DC.
45. **Rao, D., J. S. Webb, and S. Kjelleberg.** 2005. Competitive interactions in mixed-species biofilms containing the marine bacterium *Pseudoalteromonas tunicata*. Appl. Environ. Microbiol. **71:**1729–1736.
46. **Rickard, A. H., P. Gilbert, N. J. High, P. E. Kolenbrander, and P. S. Handley.** 2003. Bacterial coaggregation: an integral process in the development of multi-species biofilms. Trends Microbiol. **11:**94–100.
47. **Rocchetta, H. L., L. L. Burrows, and J. S. Lam.** 1999. Genetics of O-antigen biosynthesis in *Pseudomonas aeruginosa*. Microbiol. Mol. Biol. Rev. **63:**523–553.
48. **Romling, U., W. D. Sierralta, K. Eriksson, and S. Normark.** 1998. Multicel-

lular and aggregative behaviour of Salmonella typhimurium strains is controlled by mutations in the agfD promoter. Mol. Microbiol. **28:**249–264.

49. **Schink, B.** 2002. Synergistic interactions in the microbial world. Antonie Leeuwenhoek **81:**257–261.
50. **Spiers, A. J., J. Bohannon, S. M. Gehrig, and P. B. Rainey.** 2003. Biofilm formation at the air-liquid interface by the Pseudomonas fluorescens SBW25 wrinkly spreader requires an acetylated form of cellulose. Mol. Microbiol. **50:**15–27.
51. **Spiers, A. J., S. G. Kahn, J. Bohannon, M. Travisano, and P. B. Rainey.** 2002. Adaptive divergence in experimental populations of Pseudomonas fluorescens. I. Genetic and phenotypic bases of wrinkly spreader fitness. Genetics **161:**33–46.
52. **Sternberg, C., B. B. Christensen, T. Johansen, N. A. Toftgaard, J. B. Andersen, M. Givskov, and S. Molin.** 1999. Distribution of bacterial growth activity in flow-chamber biofilms. Appl. Environ. Microbiol. **65:**4108–4117.
53. **Thormann, K. M., R. M. Saville, S. Shukla, and A. M. Spormann.** 2005. Induction of rapid detachment in *Shewanella oneidensis* MR-1 biofilms. J. Bacteriol. **187:**1014–1021.
54. **Tolker-Nielsen, T., U. C. Brinch, P. C. Ragas, J. B. Andersen, C. S. Jacobsen, and S. Molin.** 2000. Development and dynamics of *Pseudomonas* sp. biofilms. J. Bacteriol. **182:**6482–6489.
55. **Ude, S., D. L. Arnold, C. D. Moon, T. Timms-Wilson, and A. J. Spiers.** 2006. Biofilm formation and cellulose expression among diverse environmental Pseudomonas isolates. Environ. Microbiol. **8:**1997–2011.
56. **Walsh, A. G., M. J. Matewish, L. L. Burrows, M. A. Monteiro, M. B. Perry, and J. S. Lam.** 2000. Lipopolysaccharide core phosphates are required for viability and intrinsic drug resistance in Pseudomonas aeruginosa. Mol. Microbiol. **35:**718–727.
57. **Werner, E., F. Roe, A. Bugnicourt, M. J. Franklin, A. Heydorn, S. Molin, B. Pitts, and P. S. Stewart.** 2004. Stratified growth in *Pseudomonas aeruginosa* biofilms. Appl. Environ. Microbiol. **70:**6188–6196.
58. **Wolfaardt, G. M., J. R. Lawrence, R. D. Robarts, S. J. Caldwell, and D. E. Caldwell.** 1994. Multicellular organization in a degradative biofilm community. Appl. Environ. Microbiol. **60:**434–446.
59. **Xu, K. D., P. S. Stewart, F. Xia, C. T. Huang, and G. A. McFeters.** 1998. Spatial physiological heterogeneity in *Pseudomonas aeruginosa* biofilm is determined by oxygen availability. Appl. Environ. Microbiol. **64:**4035–4039.
60. **Zampirolli, F., and R. Lotufo.** 2001. Fast multidimensional parallel Euclidean distance transform based on mathematical morphology, p. 100–105. *In* D. Borges and T. Wu (ed.), XIV Brazilian Symposium on Computer Graphics and Image Processing. IEEE Press.
61. **Zogaj, X., M. Nimtz, M. Rohde, W. Bokranz, and U. Romling.** 2001. The multicellular morphotypes of Salmonella typhimurium and Escherichia coli produce cellulose as the second component of the extracellular matrix. Mol. Microbiol. **39:**1452–1463.